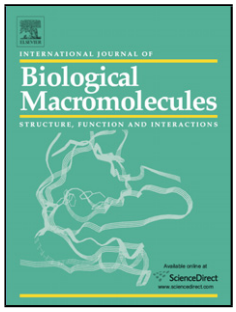

Title: A physiochemical and optical properties of chitosan based graphene oxide bionanocomposite

Author: Santosh Kumar Joonseok Koh

PII: S0141-8130(14)00491-7
DOI: http://dx.doi.org/doi:10.1016/j.ijbiomac.2014.07.019
Reference: BIOMAC 4484

To appear in: *International Journal of Biological Macromolecules*

Received date: 14-5-2014
Revised date: 15-6-2014
Accepted date: 4-7-2014

Please cite this article as: S. Kumar, J. Koh, A physiochemical and optical properties of chitosan based graphene oxide bionanocomposite, *International Journal of Biological Macromolecules* (2014), http://dx.doi.org/10.1016/j.ijbiomac.2014.07.019

A physiochemical and optical properties of chitosan based graphene oxide bionanocomposite

Santosh Kumar[a*,b] and Joonseok Koh[a*]

[a]*Department of Organic and Nano System Engineering, Konkuk University, 120 Neungdong-ro, Gwangjin-gu, Seoul 143-701, Republic of Korea.*

[b]*Departamento de Quimica, Faculdade de Ciências e Tecnologia da Universidade de Coimbra, 3004-535 Coimbra, Portugal*

Corresponding author: *E-mail: ccdjko@konkuk.ac.kr (JK); santoshics@gmail.com (SK)

Tel. /Fax: +82.2.3437.0238

ABSTRACT

In the present investigation an ecofriendly approach and a simple homogeneous solution casting method led to the development of biodegradable chitosan/graphene oxide bionanocomposites. The formation of bionanocomposite was confirmed by UV-visible, FT-IR, Raman spectroscopy, XRD, and further evaluated by thermogravimetric analysis (TGA), scanning electron microscopy (SEM) and transmission electron microscopy (TEM). The circular dichroism (CD) study of chitosan/graphene oxide revealed that the intensity of the negative transition band at wavelength of 200-222 nm in the decreased with the different pH of chitosan/graphene oxide solutions. It was also found that the pH conditions affect the interaction between chitosan and graphene oxide. Optical properties of chitosan/graphene oxide are evaluated by photoluminescence (PL) spectroscopy which showed blue shift at excitation wavelength of 255 nm compared to graphene oxide. These results strongly suggest that the

bionanocomposite materials may open new vistas in biotechnological, biosensor and biomedical applications.

***Keywords**:* Chitosan; graphene oxide; physiochemical; optical study.

1. Introduction

In recent years, there is a growing interest to develop materials with technological importance in optoelectronic devices, biological labeling and sensing [1-6]. Graphene, an allotrope of carbon arranged in a honeycomb crystal lattice into one atom thick planar sheet has attracted wide interest among the scientific community due to its fascinating high electronic, mechanical and thermal properties [7,8]. Graphene oxide (GO) obtained by exfoliation of graphite with a high yield under simple oxidizing conditions contains hydroxyl and epoxide groups on the basal planes and carboxyl or carbonyl groups mostly at the sheet edges offer unique and desirable characteristics suitable for biomedical applications [9,10]. In other hand, Chitosan is second most abundant biopolymer in nature after cellulose [11,12] on the other extreme with two types of reactive functional groups amino (NH_2) at C-2 and hydroxyl (OH) at C-3 and C-6 position on its backbone along with interdispersed acetamido groups has been used in biomedical, pharmaceutical and industrial applications due to its biodegradability, biocompatibility and low cytotoxicity [13-18]. Recently, we have demonstrated optical properties of chitosan based dye containing naphthalimide group [19]. Many researchers have modified the biopolymers with inorganic materials to improve several properties such as thermal conductivity and mechanical strength. Graphene oxide can improve the mechanical strength of the alginate/graphene oxide fibers [20]. Another

study revealed that the tensile strength of chitosan/graphene oxide composite is 1.7 times higher than that of the pure chitosan at dry state while it is 3 times higher at wet state [21]. The thermal stability and mechanical properties of the cellulose/graphene oxide composite materials are improved significantly over those of pure cellulose [22]. Recently, Li et al., [23] have developed hyaluronic acid-graphene oxide conjugates, with a high loading of photosensitizers as a cancer cell targeted and photoactivity switchable nanoplatform for photodynamic therapy. Some researchers have reported weak broad photoluminescence of graphene oxide, which was believed to originate from the carbon sp^2 domains/clusters embedded within a sp^3 matrix but it was invisible under UV irradiation [24].

Prompted by these results and in continuation of our studies herein, we report the photoluminescence (PL) and circular dichroism (CD) optical activity studies of chitosan/graphene oxide. Efforts have been made to explore the possibility of using the chitosan/graphene oxide bionanocomposite as a platform for development of optical properties for biosensor, detection of molecules and biomedical applications.

2. Experimental details

2.1. Materials and reagents

Chitosan with a degree of deacetylation (DD) of 79% was supplied by Sigma-Aldrich Chemical Co., (USA). Graphite, 30% H_2O_2, $KMnO_4$, and glacial acetic acid were purchased from Sigma-Aldrich Co., (USA). Hydrochloric acid was obtained from Samchun Pure Chemical Co. Ltd. (South Korea). H_2SO_4 was obtained from Matsunoen

Chemicals Ltd. (Osaka, Japan). Deionized water of conductivity 20 μS/cm was generated in the laboratory. All chemicals were used without further purification.

2.2. Measurement and Characterization

Fourier transform infrared (FT-IR) spectra of the compounds were recorded on a Jasco FT-IR 300E (Tokyo, Japan) using an attenuated total reflectance method for films. Powder samples were mixed with KBr and pressed into a thin pellet which was used for analysis. The Raman spectra were obtained by a Raman spectroscopy, Horiba Jobin Yvon/LabRam Aramis, laser 514 nm (Ar-ion laser), power = 0.5mW. X-ray diffraction measurements were performed using a (D/Max2500VB+/Pc, Rigaku, Japan) with a Cu Kα radiation source (wavelength λ= 0.154 nm) at a voltage of 40 kV and a current of 50 mA. The scanning rate was 3˚/min and the scanning scope of 2θ was from 2˚ to 45˚. Thermogravimetric analysis (TGA) was performed using a TA instruments Q50 thermal analyser with a nitrogen flow rate of 30 mL/min and heating rate of 10˚C/min. The surface morphology was analysed by field-emission scanning electron microscope (FE-SEM, JSM-6700F, Jeol Ltd., Japan) and High Resolution transmission electron microscope (HR-TEM, JEM 3010, Jeol Ltd., Japan). UV-visible absorption spectra were measured on an Agilent 8453 spectrophotometer (USA). Circular dichroism (CD) spectra were recorded on a JASCO J-715 spectrometer in water at room temperature. Cell length was 1.0 cm. Measurements were performed with a scanning speed of 1000 nm/min at a resolution of 1.0 nm. The spectra were corrected by subtracting the background of water and three spectra were accumulated and averaged for each sample. The pH of the solutions was determined with a HM-25R pH

Meter, DKK Toa Corporation (Japan). Fluorescence spectra were obtained on a Parkin-Elmer luminescence spectrometer (LS50B).

2.3. Synthesis

2.3.1. Synthesis of graphene oxide

Graphene oxide (GO) was prepared by the oxidation of graphite using a modified Hummers method [25,26]. In a 250 mL of round bottomed flask 3 g natural graphite was added to 69 mL of cold concentrated H_2SO_4 under stirring in an ice-bath. After that, 9 g $KMnO_4$ was added slowly into the flask under stirring in an ice-bath. The mixture was then stirred at 35°C for 2 h, then 138 ml distilled water was added slowly into the mixture and it was stirred for another 15 min below 100°C temperature. Then 420 mL of aqueous 30% H_2O_2 solution was added to the mixture. Finally, the product was filtered with 800 mL of 10% HCl aqueous solution to remove metal ions and then obtained powder was washed with distilled water. The obtained brown yellow powder of GO was dried under reduced pressure for 24 h.

2.3.2. Preparation of chitosan/graphene oxide bionanocomposite

200 mg of chitosan was dissolved into 10 mL of 1.5% aqueous acetic acid to prepare chitosan solution. The mixture was stirred continuously at room temperature for 20 h. The graphene oxide powder (0.030 g) was dispersed into 2 mL of distilled water and was treated by mild ultrasound for 30 min to forms a homogeneous solution. The graphene oxide was added in chitosan solution under stirring at 35^{o}C for 2 h followed by sonication for 2 h to ensure a homogeneous dispersion of chitosan/graphene oxide in

solution. The mixed solution was cast on glass plate to a desired thickness and dried under atmospheric conditions at room temperature for about 36 h. We have adopted different ratio of GO in chitosan/graphene oxide films (CS/GO-0.060 and CS/GO-0.120) to obtain chitosan/graphene oxide bionanocomposite films and were carefully detached from the glass plates.

3. RESULTS AND DISCUSSION

3.1. FT-IR spectroscopy

The FT-IR spectra of the pristine graphene oxide, pure chitosan, and chitosan/graphene oxide bionanocomposite are shown in Fig. 1a, b and c respectively. In the FT-IR spectra of pristine graphene oxide the absorption band (Fig. 1a) at 1724 cm^{-1} is characteristic of C=O stretching. The absorption peak at 1620 cm^{-1} is either assigned to the deformation of the OH band of the water absorbed by graphene oxide, or stretching of the aromatic C=C bond [27] and 846 cm^{-1} to the characteristic absorption peak of epoxy groups. The FT-IR characteristic peak of the chitosan film (Fig. 1b) is assigned to the stretching of intra and intermolecular O-H vibrations at 3411-3248 cm^{-1} overlapped with N-H stretch. 2950-2865 cm^{-1} corresponds to symmetric and asymmetric C-H vibrations. Amide I vibration band at 1640 cm^{-1} due to C-O stretch of acetyl group and amide II band at 1552 cm^{-1} due to N-H stretch have been observed. The absorption peak at 1062 cm^{-1} assigned to skeletal vibration of the bridge C-O stretch of glucosamine residue [28,29]. The characteristic absorption peak of the chitosan/graphene oxide films at 2878 cm^{-1} which can be assigned to the C-H asymmetric vibration due to chitosan incorporation. The new vibration band appeared at

1694 cm^{-1} due to the C=O stretching whereas the carboxylic group bands at 1724 cm^{-1} and 1221 cm^{-1} of pristine graphene oxide disappeared (Fig. 1c) [30]. When graphene oxide was added with chitosan the absorption peak at 3411-3248 cm^{-1} was broadened. The FT-IR analysis of chitosan/graphene oxide clearly indicates that the graphene oxide interacts with chitosan through intermolecular hydrogen bonds, so there should be good miscibility between graphene oxide and chitosan.

Fig.1.

3.2. Raman spectroscopy

Raman spectra can be used as a standard tool for studying characteristic effect of interactions on the molecular structure of a component present in nanocomposite materials. The intensity of the Raman spectra depended on the film thickness and therefore on the number of graphene layers. The graphene oxide in chitosan biopolymer solution was retained good dispersion in their composite film after solution casting [31]. Raman spectra of graphite, graphene oxide and chitosan/graphene oxide bionanocomposite displayed two prominent peaks at about 1349 cm^{-1} (D band) and about 1590 cm^{-1} (G band), are shown in Fig. 2a, b and c respectively. However, the band intensity ratio ($r = I_D/I_G$) for chitosan/graphene oxide (r = 1.00) shows an enhanced value compared to that for graphene oxide (r = 0.93) and graphite (r = 0.20), indicating the presence of localized sp^3 defects within the sp^2 carbon network upon reduction of the exfoliated graphene oxide.

Fig.2.

3.3. Thermogravimetric analysis

The thermal stability of the pristine graphene oxide, pure chitosan film and three different ratio of GO in chitosan/graphene oxide films (CS/GO-0.030, CS/GO-0.060 and CS/GO-0.120) were studied by thermogravimetric analysis are shown in Fig. 3. The initial weight loss of all samples at 47-100 °C, was due to evaporation of water, whereas the second stage of weight loss in the range (222-371°C) due to a complex process including the degradation of the saccharide rings [32]. The temperature of maximum loss value of CS/GO-0.030, CS/GO-0.060, and CS/GO-0.120 bionanocomposite films are similar to that of pure chitosan. The results demonstrated that the loading levels of the graphene oxide were low so that it can affect the decomposition temperature of the nanocomposite films. It also indicates that the weight percent of the film is higher relatively than that of pure chitosan, which can be attributed to the enhanced thermal stability of graphene oxide.

Fig.3.

3.4. X-ray diffraction analysis

Fig. 4 represents the structural analysis of pure chitosan film, pristine graphite, pristine graphene oxide and chitosan/graphene oxide bionanocomposites were investigated by X-ray diffraction. X-ray diffraction studies of pristine graphite exhibits very intense peak at $2\Theta = 26°$. Diffractive region of pristine graphene oxide is observed at $2\Theta = 11°$. The increase in *d*-spacing is due to the intercalation of –OH functional groups in between graphene layers. After exfoliation, the substantial shift confirms that the conversion of graphene oxide into graphite. Pure chitosan films showed a characteristic peak at around $2\Theta = 11°$ and sharp peak at 20°. The main diffractive

region of chitosan-graphene oxide is observed small peak at 2Θ = 11.28° and weak broad peak at 2Θ = 21.18°. When incorporation of graphene oxide in chitosan chemical structure of the chitosan films changes due to the overlap of biopolymer diffraction, it indicates that there were mainly physical interaction but scarcely chemical reaction between chitosan and graphene oxide [21]. The chitosan/graphene oxide bionanocomposite exhibited a combination of amorphous and crystalline peaks [33].

Fig.4.

3.5. Surface morphology

The morphology of the prepared materials was investigated by field-emission-scanning electron micrographs (FE-SEM) and high resolution transmission electron microscopy (HR-TEM) techniques. Fig. 5 shows the field-emission-scanning electron micrographs (FE-SEM) of a pure chitosan film and chitosan/graphene oxide bionanocomposite. These images indicate that the graphene oxide is uniformly dispersed in the chitosan biopolymer matrix to form a layered structure and generating large cavity (Fig. 5c and 5d). Surface morphology of pure chitosan film is nonporous, smooth membranous without any microstructures (Fig. 5a and 5b). The SEM images showed that bionanocomposite not showing porous structure because the pore sizes were gradually decreasing due to the percentage increase of graphene oxide stocking on the polymer matrix, which also indicates development of strong hydrogen bond interactions between graphene oxide and polymer. The HR-TEM images of chitosan/graphene oxide bionanocomposite are shown in Fig. 5e and 5f indicate a strong interaction between the chitosan and graphene oxide. We observed in Fig. 5e

folds and wrinkle nature at the rim of the graphene oxide due to intrinsic thermodynamically unstable properties [34]. It is clearly visible in the image that chitosan biopolymer is uniformly coated on the surface of graphene sheets.

Fig.5.

3.6. UV-Vis absorption Spectra

The UV-Vis spectra of graphene oxide and chitosan/graphene oxide are shown in Fig. 6. The graphene oxide has a characteristic peak at 235 nm due to the π-π* transition of C=C [35]. A characteristic absorption peak was observed at 270 nm after the treatment of chitosan onto the graphene oxide. The absorption peak shift of chitosan/graphene oxide is ascribed to the interaction between chitosan and graphene oxide.

Fig.6.

3.7. Circular dichroism (CD) study

The measurements of the circular dichroism spectrum of the pristine GO, pure chitosan and different acidic pH conditions of chitosan/graphene oxide in aqueous solutions are shown in Fig. 7. The non covalent molecular interactions including hydrogen bonding and hydrophobic interactions play critical roles in maintaining the highly ordered structures of biomacromolecules. The circular dichroism (CD) spectra of chitosan/graphene oxide measured using homogenious aqueous solution samples exhibit a strong negative CD band, corresponding to n→π* electronic transitions of the –NH-CO- chromophore of GlcNAc units located at about 210 nm, this band position is independent of pH and ionic strength. The results showed in Fig. 7 the intensity of CD

spectrum of pure chitosan is larger than that of the chitosan interacting with graphene oxide. The more regularly structured polymer will have a large intensity of CD spectrum [37,38]. The pristine graphene oxide didn't show circular dichroism spectrum. In order to study the optical activity of chitosan/graphene oxide over three batches of solutions were randomly taken from different pH of chitosan/graphene oxide for CD experiments. Each measurement showed chitosan interacting with graphene oxide at different acidic pH conditions like 6.31, 4.29 and 4.23, a negative Cotton effect with very strong signals at around 222 nm [39]. The chitosan-graphene oxide CD spectra could be explained by the presence of optically active forms of the graphene oxide bound to chitosan biopolymer. Muzzarelli et al [40] have reported an interaction of soluble chitosan with anionic dyes in water and Feng et al [41] have reported interaction of chitosan with multiwalled carbon nanotubes. The binding was depend on pH.

Fig.7.

3.8. Fluorescence study

The fluorescence studies of pristine graphene oxide and chitosan/graphene oxide were performed to emphasize its emission properties as shown in Fig. 8. The pristine graphene oxide had emission spectrum (λem) peak at 446, 471, 492 and 516 nm at excitation wavelength of 255 nm. The chitosan/graphene oxide had emission spectrum (λem) peak at 428 nm at excitation wavelength of 255 nm. In comparison with chitosan, we showed chitosan/graphene oxide had red-shifted emission maxima due to bandgap transitions corresponding to conjugated π-domains, and the other with more complex origins that are more or less associated with defects in the graphene structure

[42]. In comparision with pristine GO, we showed chitosan/graphene oxide had blue shifted emission maxima due to the electronic structures attributed to the polydistribution of sp^2 cluster sizes [35]. The fluorescent intensity was also controlled by the conjugation length and variation of the substituents [43,44].

Fig.8.

4. Conclusions

The biocompatible and biodegradable chitosan/graphene oxide bionanocomposites were prepared by solvent casting method and confirmed by FT-IR, Raman and X-ray diffractometry analysis. The thermal studies showed that the loading level of the graphene oxide can affect the decomposition temperature of the bionanocomposites. The morphological study of the bionanocomposite indicates that the graphene oxide is uniformly dispersed in the polymer matrix to form a layered structure. The UV-vis absorption and photoluminescence spectra showed optical properties. The circular dichroism study of chitosan/graphene oxide indicates that the interaction with chitosan and graphene oxide were in the pH range of 4 to 6. Our findings are encouraging as the chitosan/graphene oxide bionanocomposite can be used as a potential tool for biomedical applications and will play a role in biotechnology and molecular biology.

Acknowledgements

This research was supported by Konkuk University, Seoul, South Korea and FCT, Portugal.

References

[1] S. H. Wang, M. Y. Han, D. J. Huang, J. Am. Chem. Soc. 131 (2009) 11692-11694.

[2] X. Michalet, F. F. Pinaud, L. A. Bentolila, J. M. Tsay, S. Doose, J. J. Li, G. Sundaresan, A. M. Wu, S. S. Gambhir, S. Weiss, Science 307 (2005) 538-544.

[3] Y. Wang, Z. Li, J. Wang, J. Li, Y. Lin, Trend. Biotech. 29 (2011) 205-212.

[4] C. Li, J. Adamcik, R. Mezzenga, Nat. Nanotech. 7 (2012) 421-427.

[5] V. N. Mochalin, Y. Gogotsi, J. Am. Chem. Soc. 131 (2009) 4594-4595.

[6] J. Peng, W. Gao, B. K. Gupta, Z. Liu, R. R. Aburto, L. Ge, L. Song, L. B. Alemany, X. Zhan, G. Gao, S. A. Vithayathil, A. Kaipparettu, A. A. Marti, T. Hayashi, J. J. Zhu, P. M. Ajayan, Nano Lett. 12 (2012) 844-849.

[7] J. C. Meyer, A. K. Geim, M. I. Katsnelson, M. I. Novoselov, T. J. Booth, S. Roth, Nature 446 (2007) 60-63.

[8] Y. B. Zhang, Y. W. Tan, H. L. Stormer, P. Kim, Nature 438 (2005) 201-204.

[9] Y. Zhang, T. R. Nayak, H. Hong, W. Cai, Nanoscale 4 (2012) 3833-3842.

[10] C. Chung, Y. K. Kim, D. Shin, S. R. Ryoo, B. H. Hong, D. H. Min, Acc. Chem. Res. 46 (2013) 2211.

[11] R. A. A. Muzzarelli, Chitin. Pergamon Press, Oxford, UK, 1977.

[12] R. A. A. Muzzarelli, J. Boudrant, D. Meyer, N. Manno, M. D. Marchis, M. G. Paoletti, Carbohydr. Polym. 87 (2012) 995-1012.

[13] P. Garg, S. Kumar, S. Pandey, H. Seonwoo, P. Choung, J. Koh, J. H. Chung, J. Mater. Chem. B 1 (2013) 6053-6065.

[14] R. A. A. Muzzarelli, C. Muzzarelli, In Advances in Polymer Science, T. Heinze, ed. 186 (2005) 151-209. Springer Verlag, Berlin.

[15] J. M. Dang, K. W. Leong, Adv. Drug Deliv. Rev. 58 (2006) 487-499.

[16] R. Jayakumar, R. Ramachandran, V. V. Divya Rani, K. P. Chennazhi, H. Tamura, S. V. Nair, Int. J. Biol. Macromol. 48 (2011) 336-344.

[17] R. Jayakumar, Roshini Ramachandran, P. T. Sudheesh Kumar, V. V. Divya Rani, K. P. Chennazhi, H. Tamura, S. V. Nair, Int. J. Biol. Macromol. 49 (2011) 274-280.

[18] K. C. Kavya, R. Jayakumar, S. V. Nair, K. P. Chennazhi, Int. J. Biol. Macromol. 59 (2013) 255-263.

[19] S. Kumar, J. Koh, Carbohydr. Polym. 94 (2013) 221-228.

[20] Y. He, N. Zhang, Q. Gong, H. Qiu, W. Wang, Y. Liu, J. Gao, Carbohydr. Polym. 88 (2012) 1100-1108.

[21] D. Han, L. Yan, W. Chen, W. Li, Carbohydr. Polym. 83 (2011) 653-658.

[22] D. Han, L. Yan, W. Chen, W. Li, P. R. Bangal, Carbohydr. Polym. 83 (2011) 966-972.

[23] F. Li, S. J. Park, D. Ling, W. Park, J. Y. Han, K. Na, K. Char, J. Mater. Chem. B, 1 (2013) 1678-1686.

[24] G. Eda, Y. Y. Lin, C. Mattevi, H. Yamaguchi, H. A. Chen, I. S. Chen, , C. W. Chen, M. Chhowalla, Adv. Mater. 22 (2010) 505-509.

[25] W. S. Hummers, R. E. Offeman, J.Am. Chem. Soc. 80 (1958) 1339-1339.

[26] C. Hou, Q. Zhang, M. Zhu, Y. Li, H. Wang, Carbon 49 (2011) 47-53.

[27] Q. Zhuang, X. Liu, Q. Wang, X. Liu, J. Zhou, Z. Han, J. Mater. Chem. 22 (2012) 12381-12388.

[28] A. Khan, R. A. Khan, S. Salmieri, C. L. Tien, B. Riedl, J. Bouchard, G. Chauve, V. Tan, M. R. Kamal, M. Lacroix, Carbohydr. Polym. 90 (2012) 1601-1608.

[29] S. Kumar, P. K. Dutta, P. Sen, Carbohydr. Polym. 80 (2010) 564-570.

[30] N. B. Colthup, L. Daly, S. E. Weberley, Introduction to Infrared and Raman Spectroscopy, 3rd ed. Academic Press, New York, USA, 1990.

[31] H. Fan, L. Wang, K. Zhao, N. Li, Z. Shi, Z. Ge, Z. Jin, Biomacromolecules 11 (2010) 2345-2351.

[32] A. P. Mathew, A. Dufresne, Biomacromolecules 3 (2002) 1101-1108.

[33] A. Bodin, L. Ahrenstedt, H. Fink, H. Brumer, B. Risberg, P. Gatenholm, Biomacromolecules 8 (2007) 3697-3704.

[34] J. Meyer, A. Geim, M. Katsnelson, K. Novoselov, D. Obergfell, S. Roth, C. Girit, A. Zettl, Solid State Commun. 143 (2007) 101-109.

[35] Q. Mei, K. Zhang, G. Guan, B. Liu, S. Wang, Z. Zhang, Chem. Commun. 46 (2010) 7319-7321.

[36] Y. Miura, K. Yasuda, K. Yamamoto, M. Koike, Y. Nishida, K. Kobayashi, Biomacromolecules 8 (2007) 2129-2134.

[37] X. Y. Gao, G. M. Xing, Y. L. Yang, X. L. Shi, R. Liu, W. G. Chu, L. Jing, F. Zhao, C. Ye, H. Yuan, X. H. Fang, C. Wang, Y. L. Zhao, J. Am. Chem. Soc. 130 (2008) 9190-9191.

[38] S. Kumar, J. Koh, J. Appl. Polym. Sci. 124 (2012) 4897-4903.

[39] S. Kumar, J. Koh, Int. J. Molecul. Sci. 13 (2012) 6102-6116.

[40] S. Stefancich, F. Delben, R. A. A. Muzzarelli, Carbohydr. Polym. 24 (1994) 17-23.

[41] W. Feng, Y. Li, P. Ji, Am. Inst. Chem. Eng. J. 58 (2012) 285-291.

[42] L. Cao, M. J. Meziani, S. Sahu, Y. P. Sun, Acc. Chem. Res. 46 (2013) 171-180.

[43] S. Kumar, P. K. Dutta, J. Koh, Int. J. Biol. Macromol. 49 (2011) 356-361.

[44] S. Kumar, J. Koh, Int. J. Biol. Macromol. 51 (2012) 1167-1172.

Figure Captions

Fig.1. FTIR of pristine graphene oxide (a), pure chitosan (b) and chitosan/graphene oxide bionanocomposite (c).

Fig.2. Raman spectra of graphite (a), pristine graphene oxide (b), and chitosan/graphene oxide bionanocomposite (c).

Fig.3. TGA of pristine graphene oxide (a), pure chitosan film (b) and chitosan/graphene oxide 0.030 (c), 0.060 (d) and 0.120 (e) bionanocomposite.

Fig.4. XRD of pure chitosan film (a), pristine graphene oxide (b), graphite (c) and chitosan/graphene oxide bionanocomposite (d).

Fig.5. SEM images of pure chitosan film (a and b), chitosan/graphene oxide bionanocomposite (c and d) and TEM images of chitosan/graphene oxide bionanocomposite (e and f).

Fig.6. UV-visible spectra of pristine graphene oxide (a) and chitosan/graphene oxide (b).

Fig.7. CD spectra of pristine graphene oxide (a) pure chitosan (b), chitosan/graphene oxide at pH 6.31 (c), 4.29 (d) and 4.20 (e).

Fig.8. PL spectra of pristine graphene oxide (a) and chitosan/graphene oxide (b) at excitation wavelength of 255 nm.

Figure(1)

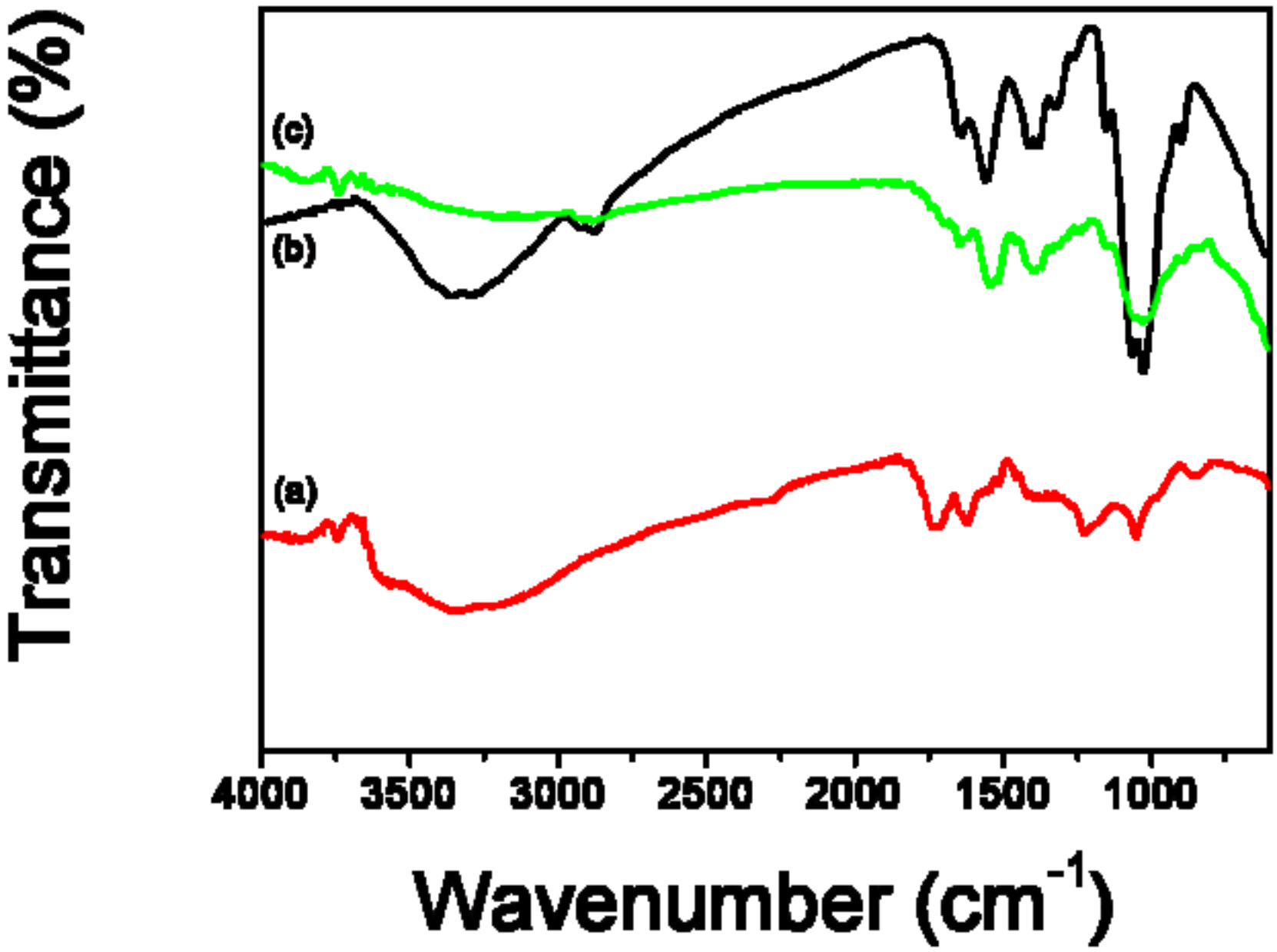
Transmittance (%)
(c)
(b)
(a)
4000
3500
3000
2500
2000
1500
1000
Wavenumber (cm-1)

Figure(2)

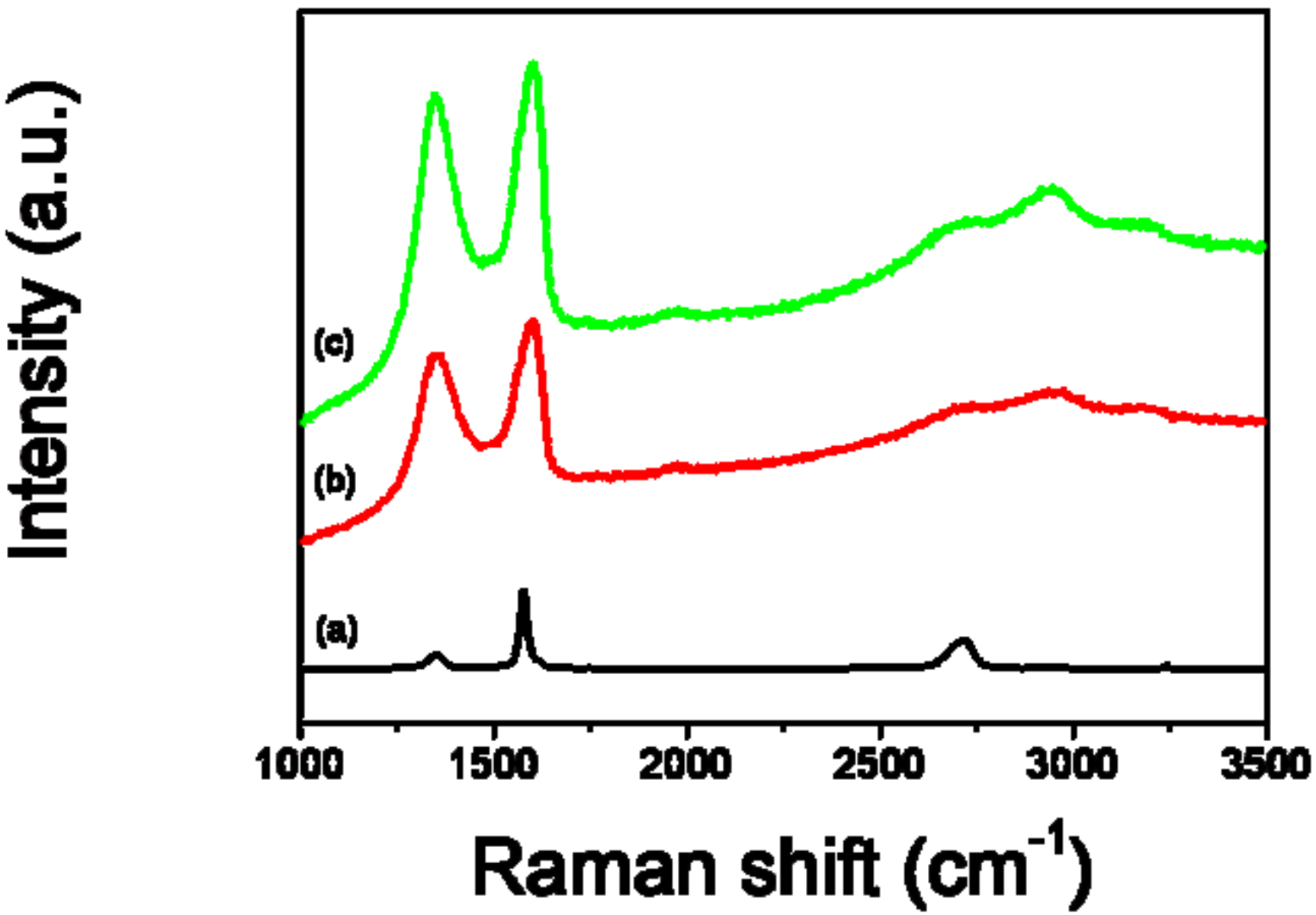
Intensity (a.u.)
(c)
(b)
(a)
1000
1500
2000
2500
3000
3500
Raman shift (cm-1)

Figure(3)

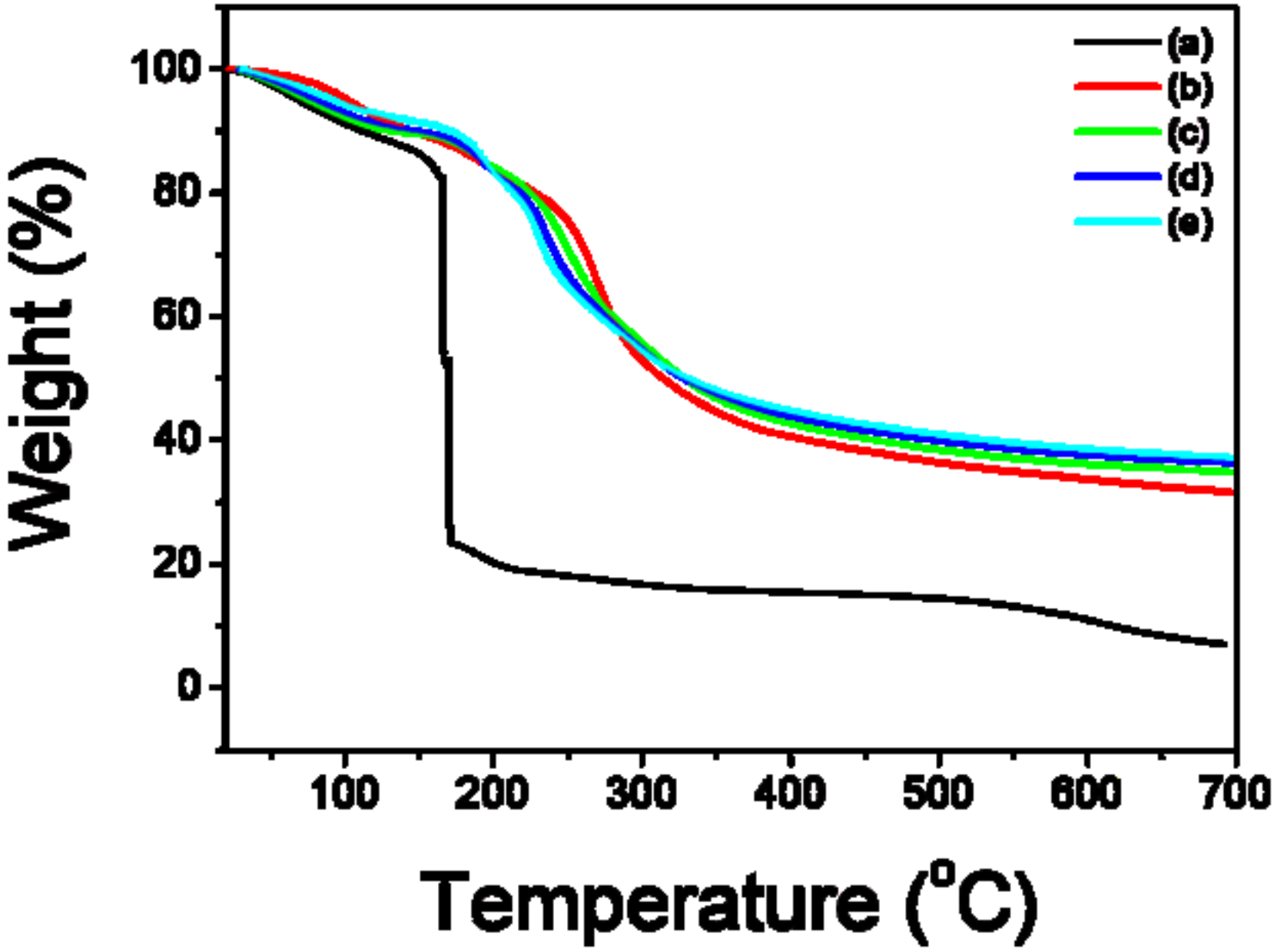
Weight (%)
100
80
60
40
20
0
100
200
300
400
500
600
700
Temperature (°C)
(a)
(b)
(c)
(d)
(e)

Figure(4)

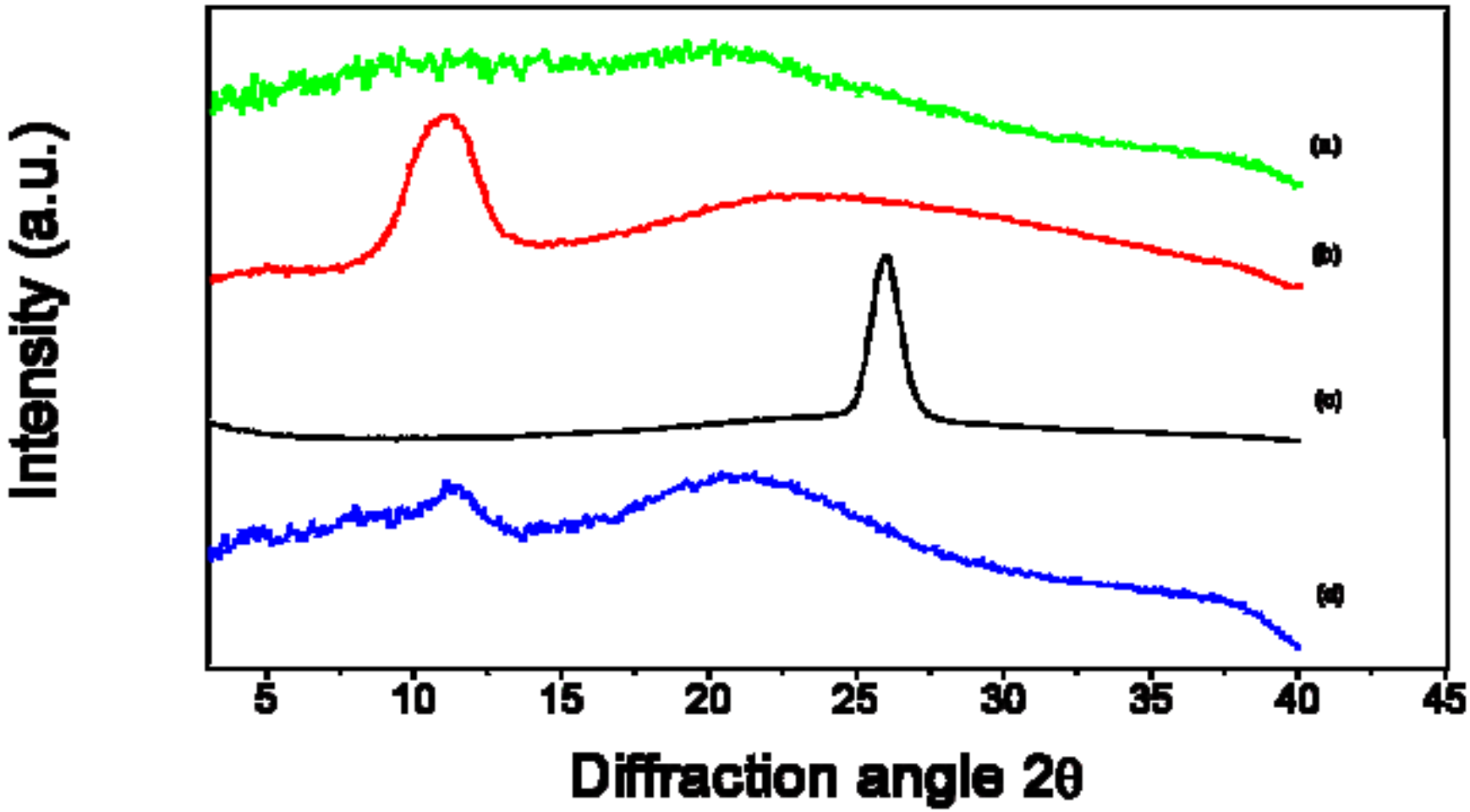
Intensity (a.u.)
(a)
(b)
(c)
(d)
5
10
15
20
25
30
35
40
45
Diffraction angle 2θ

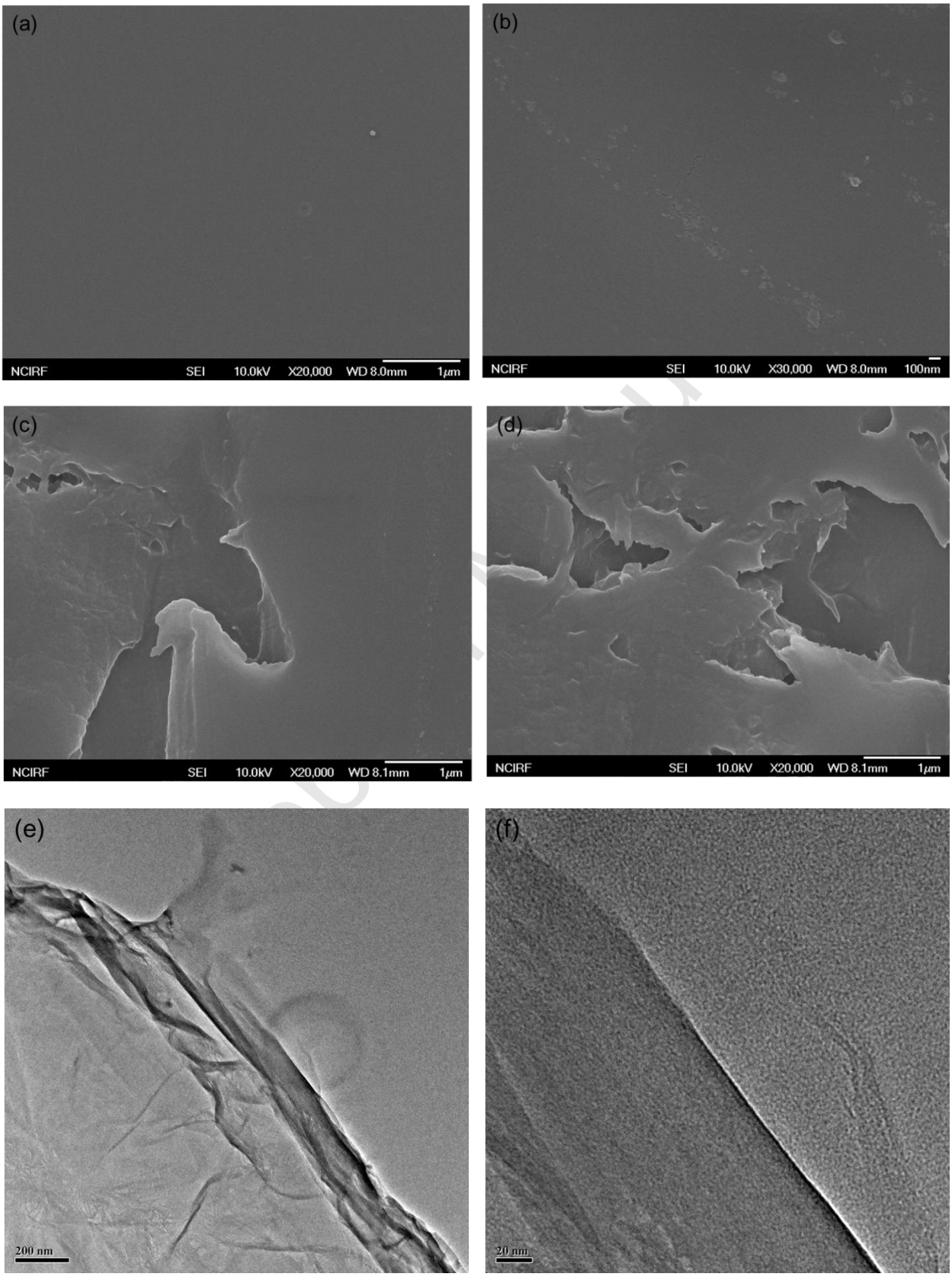

Figure(6)

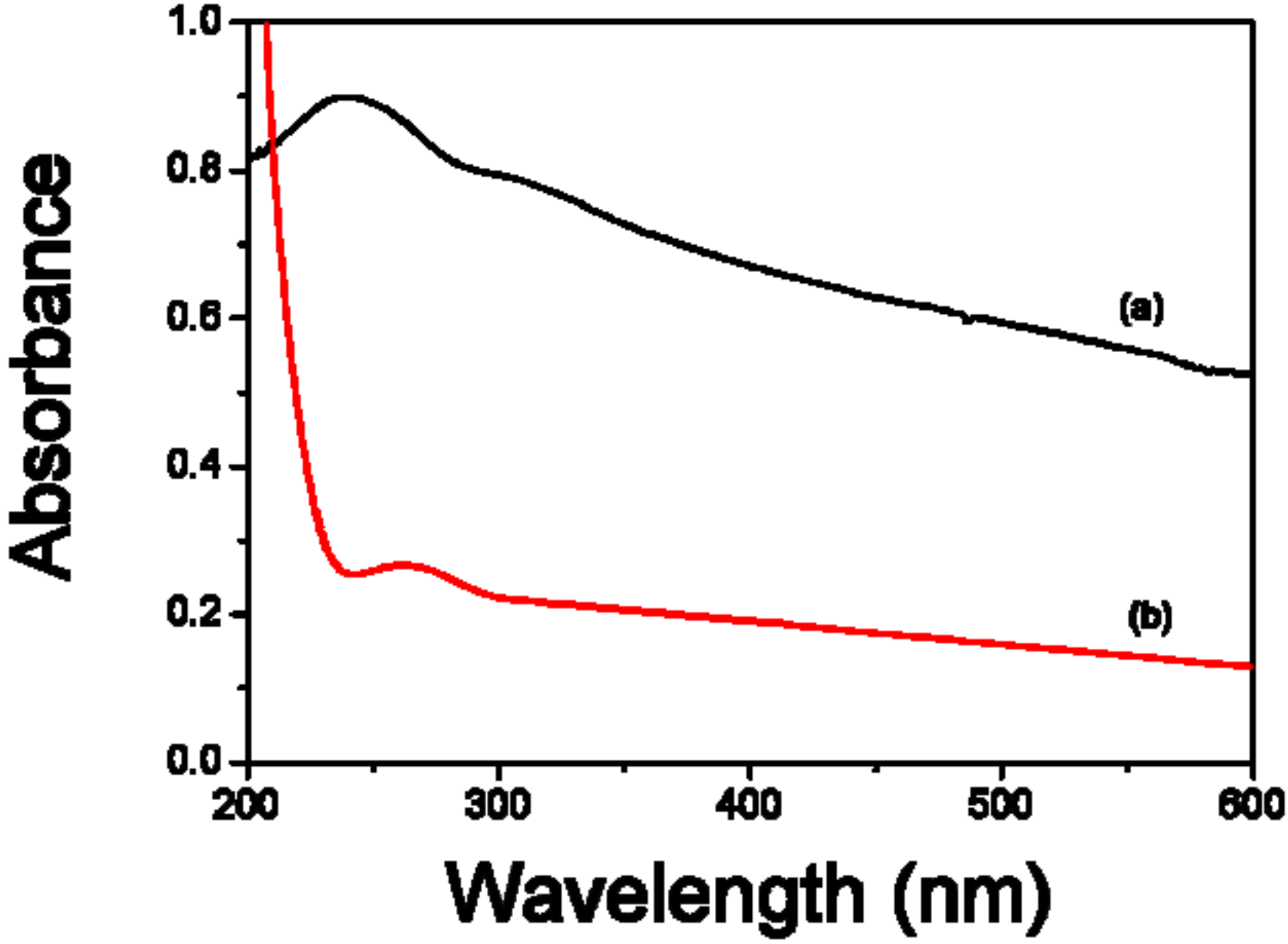
Absorbance
1.0
0.8
0.6
0.4
0.2
0.0
200
300
400
500
600
Wavelength (nm)
(a)
(b)

Figure(7)

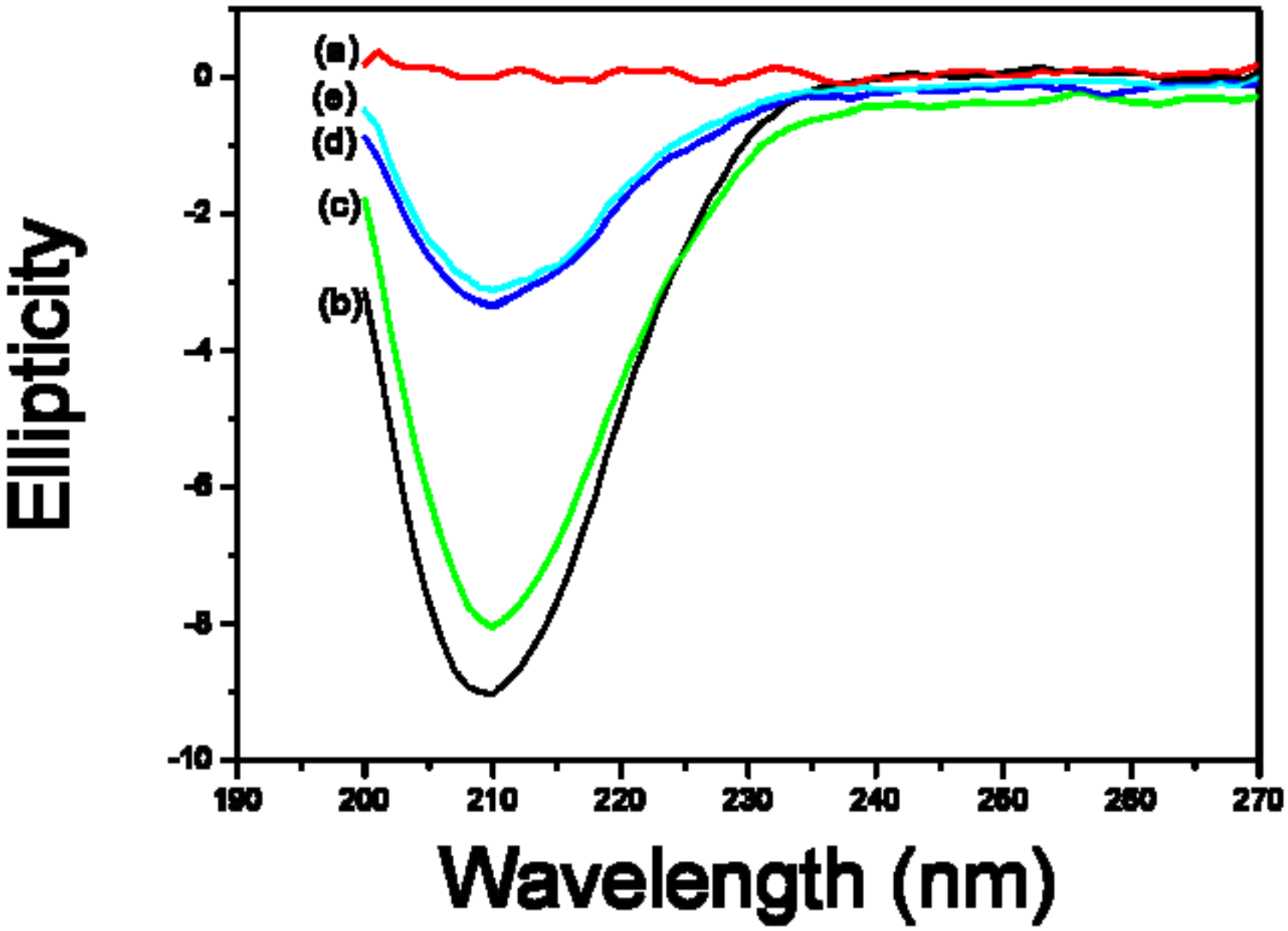
(a)
(e)
(d)
(c)
(b)
0
-2
-4
-6
-8
-10
190
200
210
220
230
240
250
260
270
Ellipticity
Wavelength (nm)

Figure(8)

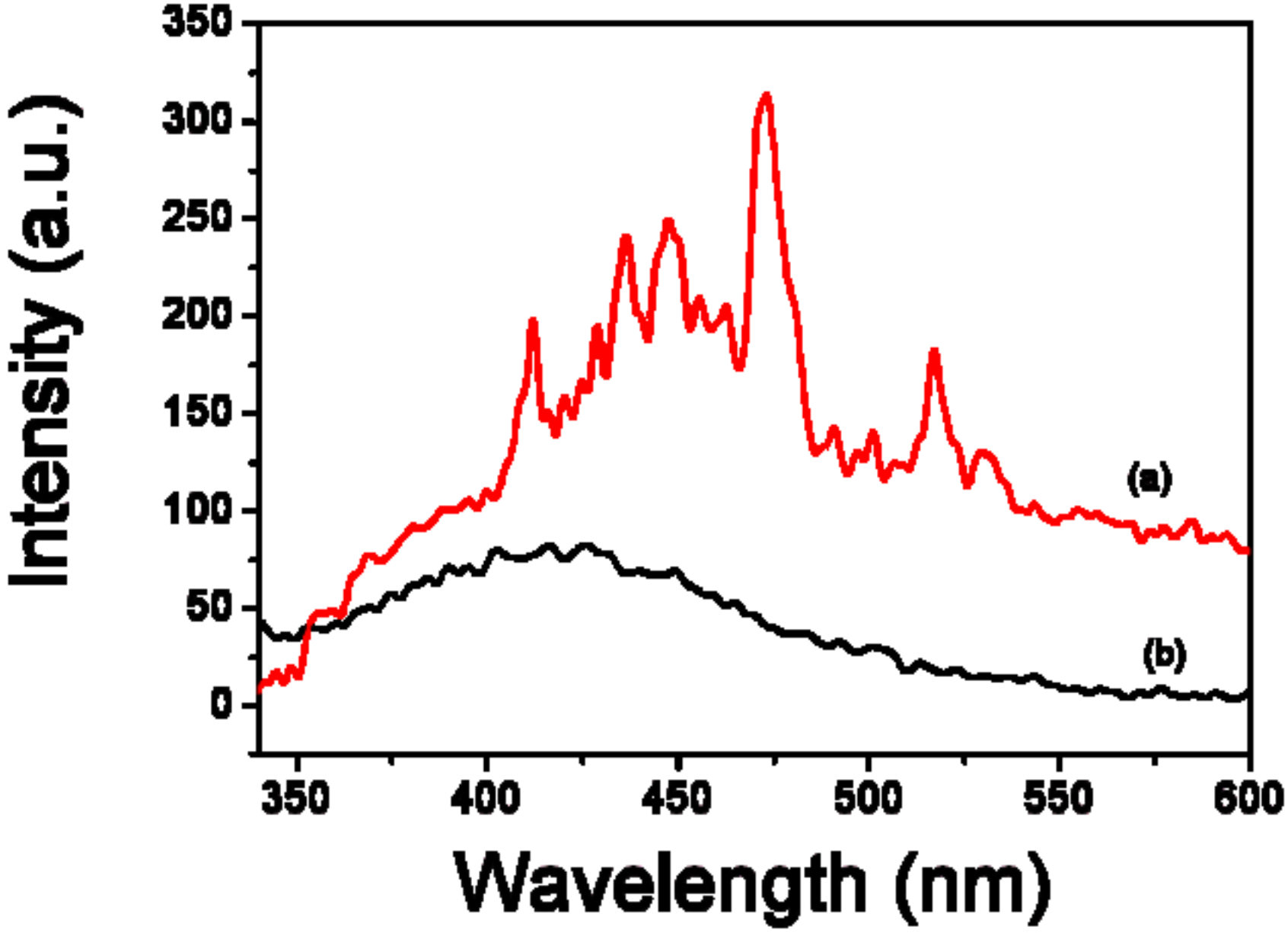
Intensity (a.u.)
350
300
250
200
150
100
50
0
350
400
450
500
550
600
Wavelength (nm)
(a)
(b)

Figure graphical abstract revised

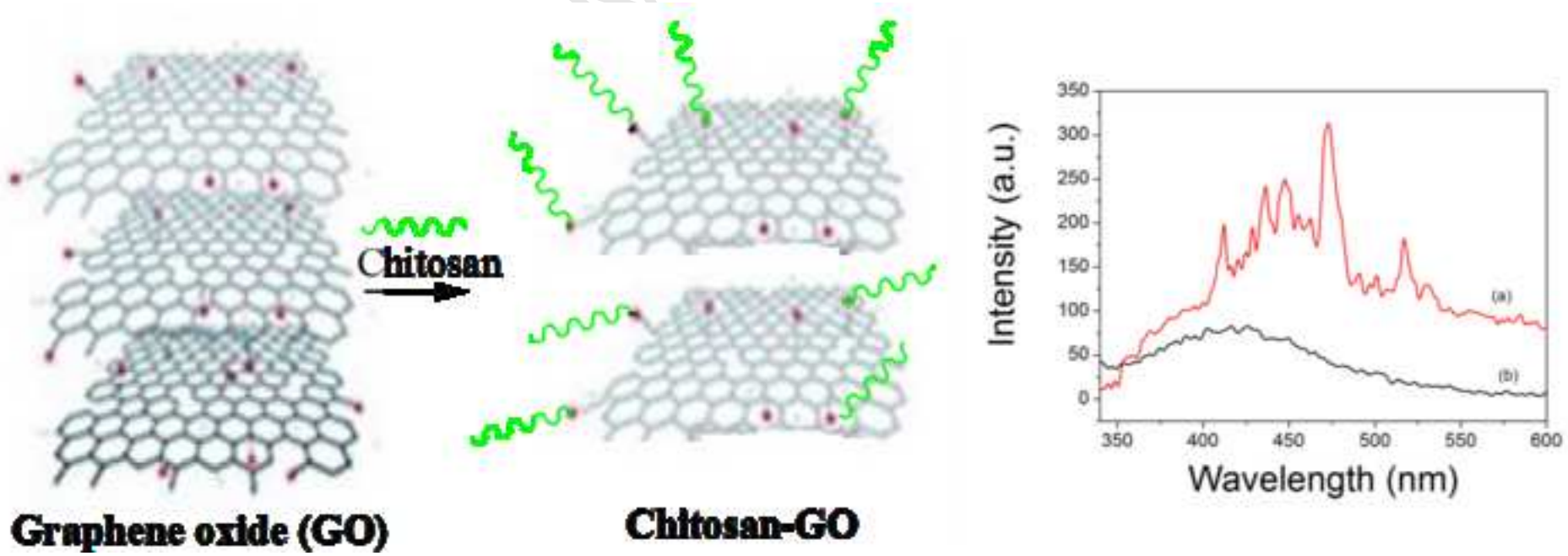

Highlights

- Preparation and advanced techniques characterization of the bionanocomposite.
- Morphological study showed that the graphene oxide is uniformly dispersed in the polymer matrix.
- UV-vis and photoluminescence spectra showed optical properties.
- Circular dichroism indicates the pH conditions affect the interaction of chitosan and graphene oxide.